AGU PUBLICATIONS

JGR

Journal of Geophysical Research: Oceans

RESEARCH ARTICLE

10.1002/2014JC010634

A modeling study of physical controls on hypoxia generation in the northern Gulf of Mexico

Liuqian Yu[1], Katja Fennel[1], and Arnaud Laurent[1]

[1]Department of Oceanography, Dalhousie University, Halifax, Nova Scotia, Canada

Key Points:
- Simple oxygen parameterization predicts hypoxia on the Louisiana shelf
- Magnitude of river discharge and wind stress are key factors affecting hypoxia
- Simple oxygen model may be sufficient for short-term hypoxia prediction

Supporting Information:
- Supporting Information S1

Correspondence to:
L. Yu,
liuqian.yu@dal.ca

Citation:
Yu, L., K. Fennel, and A. Laurent (2015), A modeling study of physical controls on hypoxia generation in the northern Gulf of Mexico, *J. Geophys. Res. Oceans*, *120*, 5019–5039, doi:10.1002/2014JC010634.

Received 10 DEC 2014
Accepted 19 JUN 2015
Accepted article online 23 JUN 2015
Published online 18 JUL 2015

Abstract The Louisiana shelf (LA shelf) in the northern Gulf of Mexico experiences hypoxic conditions every summer due to the combination of eutrophication and strong water column stratification. Here we use a three-dimensional circulation model coupled with a simple oxygen model to examine the physical controls on hypoxia generation on the LA shelf. The model assumes a constant oxygen utilization rate in the water column and a sediment oxygen consumption rate that depends on the bottom water oxygen concentration and temperature. Despite its simplicity, the model reproduces the observed variability of dissolved oxygen and hypoxia on the LA shelf, highlighting the importance of physical processes. Model results demonstrate that both river discharge and wind forcing have a strong effect on the distribution of the river plume and stratification, and thereby on bottom dissolved oxygen concentrations and hypoxia formation on the LA shelf. The seasonal cycle of hypoxia is relatively insensitive to the seasonal variability in river discharge, but the time-integrated hypoxic area is very sensitive to the overall magnitude of river discharge. Changes in wind speed have the greatest effect on the simulated seasonal cycle of hypoxia and hypoxic duration, while changes in wind direction strongly influence the geographic distribution of hypoxia. Given that our simple oxygen model essentially reproduces the evolution of hypoxia simulated with a full biogeochemical model and that physical processes largely determine the magnitude and distribution of hypoxia, a full biogeochemical model might not be necessary for short-term hypoxia forecasting.

1. Introduction

The Louisiana shelf (LA shelf) in the northern Gulf of Mexico receives large amounts of freshwater and nutrients from the Mississippi/Atchafalaya River System. The freshwater discharge enhances the vertical water column stratification in summer, limiting the oxygen supply to near-bottom waters from above [*Wiseman et al.*, 1997]. The nutrient inputs stimulate primary production, leading to high sedimentation fluxes of organic matter and significant microbial consumption of oxygen below the pycnocline. The combined effects of water column stratification and nutrient-enhanced primary production lead to the recurring development of near-bottom hypoxia (oxygen concentrations < 2 mg L^{-1} or 62.5 mmol m^{-3}) on the LA shelf every summer [*Rabalais et al.*, 2007; *Bianchi et al.*, 2010].

Retrospective analysis [*Obenour et al.*, 2013] and statistical regression models [*Forrest et al.*, 2011] show an increasing trend in the areal extent of hypoxia over the LA shelf from 1985 to 2011. It is generally accepted that this increase in hypoxic extent is mainly driven by rising anthropogenic nutrient inputs from the watershed. However, statistical regressions using nutrient load as the only independent variable do not explain the majority of interannual variability in hypoxia; when physical factors are included a much larger fraction of the variability can be explained [*Forrest et al.*, 2011; *Feng et al.*, 2012]. *Forrest et al.* [2011] found that nitrogen load alone explains only 24% of the variability in observed hypoxic area (from 1985 to 2014) whereas including the east-west wind in addition to the nitrogen load explains 47% of the variability. *Feng et al.* [2012] demonstrated that for the 1985–2010 and 1993–2010 hurricane-exclusive periods, May–June nitrate load correlates with the observed hypoxic area at $r^2 = 0.36$ and $r^2 = 0.24$, respectively. Including May–June nitrate load and the duration of upwelling favorable (eastward) wind improves the statistical relationships for both periods to $r^2 = 0.69$ and $r^2 = 0.74$, respectively. A geostatistical modeling study by *Obenour et al.* [2012] suggests that both river nutrient concentration and stratification play substantial and comparable roles in the year-to-year variability of hypoxia in the northern Gulf of Mexico. A more recent mechanistic modeling study by *Obenour et al.* [2015] found that, while seasonal nutrient loading remains an important driver of hypoxia, stratification (presented as a function of river discharge, summer east-west wind velocity,

and wind stress) contributes to a larger extent to the interannual variability in hypoxia than indicated in their previous empirical modeling study [*Obenour et al*., 2012], especially on the western LA shelf.

While the statistical modeling studies are instructive, they can only prove correlation not causation. Coupled physical-biogeochemical models are important complements that help build mechanistic understanding of the processes underlying hypoxia development and variability [*Fennel et al*., 2011, 2013; *Feng et al*., 2013; *Laurent and Fennel*, 2014; *Yu et al*., 2015; *Justić and Wang*, 2014]. While the fully coupled physical-biogeochemical models can mechanistically elucidate the complex interactions of physical and biological processes, they can be difficult to calibrate and their results are sometimes difficult to interpret. An intermediate approach is to couple a detailed hydrodynamic model with a simple parameterization of biogeochemical processes. This approach has been used successfully in Chesapeake Bay where physical forces play an important role in the development of seasonal hypoxia. For example, *Scully* [2013] implemented a very simple empirical dissolved oxygen parameterization (assuming a constant oxygen consumption rate in the water column) in a three-dimensional circulation model to examine the role of physical forcing on hypoxia in Chesapeake Bay. Despite its simplicity, the model skillfully reproduces the observed variability of dissolved oxygen and hypoxic volume in the Bay.

Motivated by these previous studies, we assess whether very simple oxygen parameterizations coupled with the hydrodynamic model we have used in our previous, fully coupled modeling studies [*Fennel et al*., 2011, 2013; *Laurent et al*., 2012; *Feng et al*., 2013; *Laurent and Fennel*, 2014; *Yu et al*., 2015] can simulate hypoxic conditions in the northern Gulf of Mexico. We find this to be the case and then use the simplified model to evaluate the role of different physical forcing factors in hypoxia formation, including river discharge, wind speed, and the seasonal shift in wind direction from upwelling-favorable in summer to downwelling-favorable during the rest of the year.

The manuscript is organized as follows. In section 2, we describe the models used in this study including a validation of the simple oxygen models against available observations and outputs from our fully coupled physical-biogeochemical model. In section 3, we examine how variations in river discharge, wind speed, and wind direction change the distribution of river plume, stratification, and thereby the extent and geographic distribution of hypoxia. Our main conclusions, given in section 5, are that our simple oxygen parameterization coupled with a realistic hydrodynamic model realistically simulates hypoxic conditions on the LA shelf, and that river discharge, wind speed, and wind direction can all significantly influence the distribution of the river plume and stratification, and thereby the bottom oxygen concentrations and hypoxia development on the LA shelf. The ability of our simple oxygen model to closely reproduce the hypoxia evolution of the full biogeochemical model, and the determining role of physical processes in hypoxia generation lead us to conclude that a full biogeochemical model may not be necessary for short-term hypoxia forecasting on the LA shelf.

2. Methods

2.1. Physical Model

Our physical model is the Regional Ocean Modelling System [*Haidvogel et al*., 2008; ROMS, http://myroms.org] configured for the Mississippi/Atchafalaya outflow region as described in *Hetland and DiMarco* [2008, 2012]. The model domain covers the Louisiana continental shelf with a horizontal resolution ranging from ~20 km in the southwestern corner to ~1 km near the Mississippi Delta (Figure 1). The model has 20 terrain-following vertical layers with increased resolution near the surface and bottom. An average profile of temperature and salinity, based on historical hydrographic data [*Boyer et al*., 2006] and assumed to be horizontally uniform, is used as physical boundary condition. At the three open boundaries, gradient conditions are used for the free surface, radiation conditions for the three-dimensional velocities, and a *Flather* [1976] condition with no mean barotropic background flow for the two-dimensional velocities. Atmospheric forcing uses 3 hourly winds from the NCEP North American Regional Reanalysis (NARR) and climatological surface heat and freshwater fluxes from *da Silva et al*. [1994a, 1994b]. Freshwater inputs from the Mississippi and Atchafalaya rivers were based on daily measurements of transport by the US Army Corps of Engineers at Tarbert Landing and Simmesport, respectively.

The physical model realistically captures the two distinct modes of circulation over the LA shelf: an upcoast circulation mode during the dominantly upwelling-favorable (westerly) winds in summer (June–August)

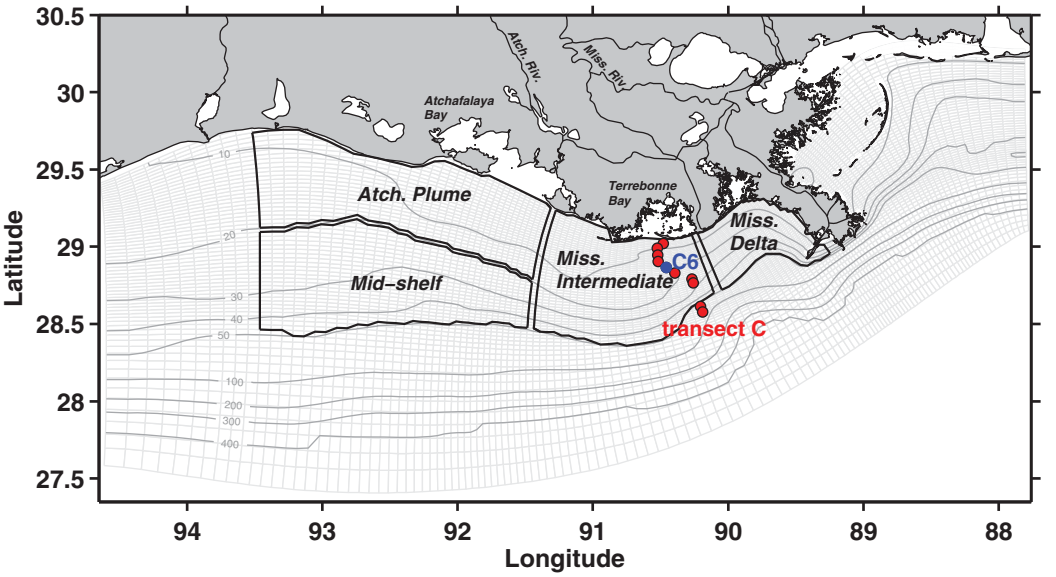

Figure 1. Model grid (light gray lines) and bathymetry (dark gray lines). The black boxes indicate selected subregions for averaging: Mississippi delta, Mississippi Intermediate, Atchafalaya Plume, and Mid-shelf region. Also shown are the stations on transect C (dots) from nearshore to offshore which represent stations C2, C3, C4, C5, C6 (blue dot), C7, C8, C9, C10, and C11.

versus westward flow during the dominantly downwelling-favorable (easterly) winds for the rest of the year [*Hetland and DiMarco*, 2008]. The skill assessment by *Hetland and DiMarco* [2012] shows that the physical model is able to faithfully reproduce the observed broad-scale features and seasonal patterns of the Mississippi/Atchafalaya River plume system and hence can be considered a reasonable hydrodynamic foundation for regional biogeochemical models.

2.2. Oxygen Models

We implemented three relatively simple oxygen models with different prescriptions of oxygen sinks in the water column and sediment within the three-dimensional circulation model. All models use the same parameterization of air-sea gas exchange ($F_{air-sea}$, in units of mmol O_2 m^{-2} d^{-1}) following *Fennel et al.* [2013] which acts on the top layer of the model:

$$F_{air-sea} = \frac{vk_{O2}}{\Delta z}\left(Ox_{sat} - Ox\right). \tag{1}$$

Here Ox and Ox_{sat} are the oxygen concentration and concentration at saturation, respectively, Δz is the thickness of the respective grid box, and vk_{O2} is the gas exchange coefficient for oxygen based on *Wanninkhof* [1992], given as:

$$vk_{O2} = 0.31\ u_{10}^2 \sqrt{\frac{660}{Sc_{Ox}}}. \tag{2}$$

u_{10} is the wind speed at 10 m above the sea surface, and Sc_{Ox} is the Schmidt number, calculated as in *Wanninkhof* [1992].

The first simple oxygen model has sinks in both water column and sediment. A net water respiration rate (NWR, in units of $mmol\ O_2\ m^{-3}d^{-1}$) is prescribed in the water column that is constant in time and spatially varying with bathymetry (h, in units of m, with a minimum at 5 m in the model). The functional form, shown in Figure 2, is a fit to the mean NWR observations for different isobath bins. Observations are calculated from data in *Murrell et al.* [2013b] by converting the net metabolism values in their Figure 5b (solid circles) to volumetric units. The NWR data set includes 341 measurements collected in spring, summer, and fall from 2003 to 2007 at multiple sites across the LA shelf. The observations did not show seasonal or alongshelf variability, but there is a cross-shelf gradient with negative NWR (indicating that primary production exceeds biological oxygen consumption in the water column) in shelf regions shallower than 20 m and positive NWR (indicating that biological consumption of oxygen exceeds primary production) deeper than

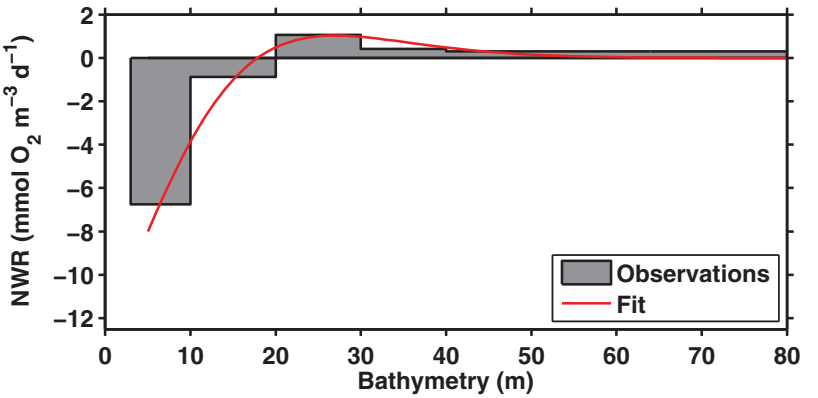

Figure 2. Fitted net water column respiration rate (NWR) based on observations of *Murrell et al.* [2013b].

20 m (as shown by the gray bars in Figure 2). Our functional form of NWR captures this cross-shelf variability and is given as:

$$NWR = 30\ \left[mmol\ O_2\ m^{-3}d^{-1}\right] * \sin\left(-15.29 + \frac{-h^{1.043}}{48.32[m]}\right) * \exp\left(-\frac{h^{1.587}}{99.95[m]}\right), \quad \text{where} \quad h \geq 5m. \tag{3}$$

In addition a temperature and oxygen-dependent sediment oxygen consumption (SOC) rate is implemented in the model, drawing down oxygen in the bottom-most grid cell [*Hetland and DiMarco*, 2008] according to:

$$SOC = 6\ \left[mmol\ O_2\ m^{-2}d^{-1}\right] * 2^{T/10^{\circ}C} * \left(1 - \exp\left(-\frac{Ox}{30[mmol\ O_2\ m^{-3}]}\right)\right), \tag{4}$$

where T (°C) and Ox (mmol O_2 m^{-3}) are the temperature and oxygen concentrations in the bottom water, respectively. We will refer to this model as NWR+SOC.

To examine the sensitivity of hypoxia to different prescriptions of oxygen sinks in water column and sediment, we ran two additional simple oxygen models in which either water column respiration or the sediment oxygen sink is turned off. These two models are denoted as "SOC only" (without NWR) and "NWR only" (without SOC), respectively. An overview of all models is given in Table 1.

We evaluate the performance of the three simple oxygen models, which were ran from 1 January 2004 to 31 December 2007, by comparing the simulated hypoxic extent and oxygen concentrations with available observations from *Rabalais et al.* [2007], *Murrell et al.* [2013a], *Nunnally et al.* [2013], and the Mechanisms Controlling Hypoxia (MCH) program. Considering that observations are spatially and temporally limited, we extended the validation by comparing output from the simple oxygen models to that of our full physical-biogeochemical model, which has been shown to realistically reproduce the observed oxygen dynamics on the LA shelf [*Yu et al.*, 2015]. Detailed parameterization and validation of the full biogeochemical model are described in *Fennel et al.* [2011, 2013], *Laurent et al.* [2012], *Laurent and Fennel* [2014], and *Yu et al.* [2015].

2.3. Model Experiments

Based on the validation of the simple oxygen models against available observations and output from our full physical-biogeochemical model (see Results section), we choose the NWR+SOC model to conduct

Table 1. Overview of Models

Model	Description
Full biogeochemical model (Full)	Realistic hydrodynamic model coupled with N-cycle model.
NWR+SOC model	Realistic hydrodynamic model coupled with simple DO parameterization where oxygen utilization rate in the water column is constant and sediment oxygen consumption rate is a function of bottom water oxygen and temperature.
SOC only model	Turn off the water column oxygen sink in the NWR+SOC model.
NWR only model	Turn off the sediment oxygen sink in the NWR+SOC model.

Table 2. Overview of Model Experiments

Experiment	Description
Baseline	Baseline run with realistic river discharge and wind forcing in year 2007.
River discharge runs	
Const RD	River discharge is set to annual average value.
High RD	Double the river discharge.
Low RD	Halve the river discharge.
Wind runs	
UF	Winds from mid July to mid August (upwelling-favorable wind) were repeated each month of the year.
DF	Winds from January (downwelling-favorable wind) were repeated each month of the year.
High UF	The repeated upwelling-favorable wind magnitude was increased to be comparable to January upwelling favorable wind.
Low DF	The repeated downwelling-favorable wind magnitude was decreased to be comparable to summer upwelling favorable wind.

sensitivity experiments that examine the effects of river discharge, wind speed, and wind direction on the extent and geographic distribution of hypoxia.

The NWR+SOC model was first run with realistic river discharge and wind forcing (denoted as "Baseline" simulation). Sensitivity experiments with varying river or wind forcing were then conducted and are compared with the baseline model experiment to evaluate the role of river discharge and wind forcing on the seasonal cycle of hypoxia (Table 2). We focus our detailed analysis of model experiments on the year 2007, which is an average year in terms of the hypoxic extent, freshwater discharge, and duration of upwelling-favorable (westerly) wind in summer.

The freshwater discharge from the Mississippi River varies considerably on both seasonal and interannual time scales (Figure 3). The discharge magnitude typically increases from winter to spring and then decreases to a minimum in summer. To evaluate the role of the seasonal variation in river discharge (RD) on the hypoxic area, we conducted a sensitivity experiment (denoted as "Const RD") where river discharge was set to the annual average value throughout the year. To examine the role of the magnitude of river discharge, we conducted High RD and low RD experiments where the event-scale variability in river discharge is preserved but the magnitude was doubled or halved, respectively. These changes in river discharge are mostly within the long-term (1983–2007) range of annual river discharge data, except in winter months and July when the increased river discharge exceeds the high end, and in spring, October and December when the decreased river discharge is below the low end of the range (Figure 3).

Wind speed and wind direction over the LA shelf also have pronounced seasonal variability, namely low magnitude and dominantly upwelling-favorable direction (westerly) in summer (June–August) and relatively high magnitude and downwelling-favorable direction (easterly) during the rest of the year (Figure 4). To evaluate the role of this seasonal change in wind forcing, we conducted an upwelling-favorable wind run (denoted as "UF") where the mid-July to mid-August upwelling-favorable wind was repeated each month of the year, and a downwelling-favorable wind run (denoted as "DF") where the downwelling-favorable wind from January was repeated each month of the year. To further examine the respective effects of wind speed

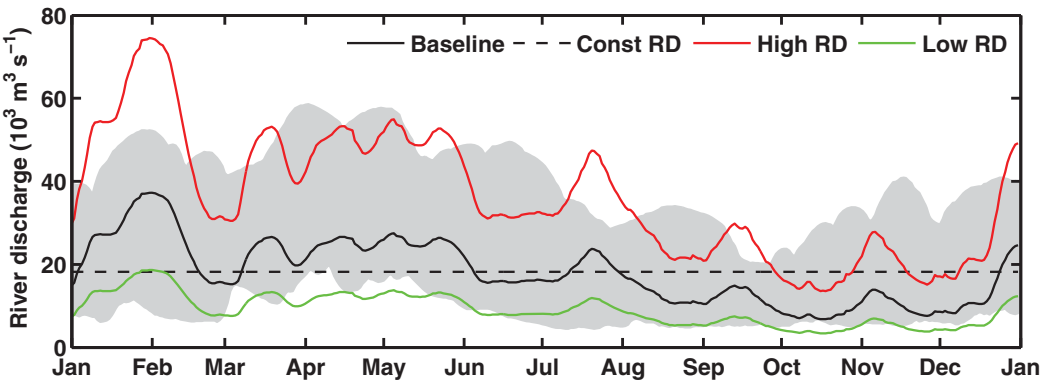

Figure 3. Mississippi and Atchafalaya River freshwater discharge. The shaded area indicates the range of annual river discharge from 1983 to 2010.

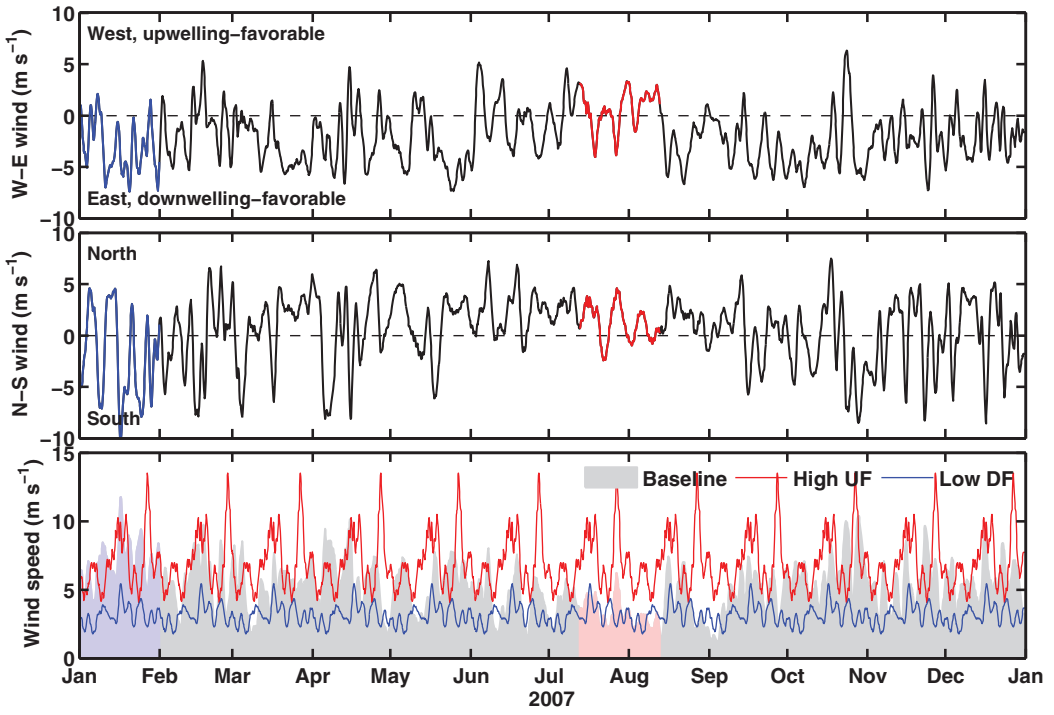

Figure 4. (a) NARR W-E wind and (b) NARR N-S wind averaged over the shelf (subregions in Figure 1). The blue and red lines indicate the January wind and 13 July to 12 August wind repeated throughout the year for DF and UF scenarios, respectively. (c) NARR wind speed in baseline run (gray shadow) and wind speed used in High UF (thin red line) and Low DF (thin blue line) scenarios. Values are averaged over the shelf (subregions in Figure 1). The blue and red shaded area indicate the January wind speed and 13 July to 12 August wind speed repeated throughout the year for DF and UF scenarios, respectively.

and wind direction, we conducted a "High UF" wind run where the wind speed from the UF run was increased (by ~2.2 times) to be comparable in terms of strength to the downwelling-favorable wind in the DF run, and a "Low DF" wind run where the wind speed from the DF run was decreased (by ~46%) to be comparable in strength to the upwelling-favorable wind from the UF run. Hence one can assess the effects of wind speed by comparing UF and High UF or DF and Low DF runs, and evaluate the effects of wind direction by comparing the UF and Low DF, or High UF and DF. Although not realistic, these simulations provide insight into the impacts of wind speed and direction on the seasonal cycle of hypoxic area.

We quantify the hypoxic extent by calculating the total area of water that has bottom dissolved oxygen concentrations below a threshold value. To represent different degrees of hypoxia, four different threshold values are used: 0.5 mg L^{-1} (anoxic), 1 mg L^{-1} (strongly hypoxic), 2 mg L^{-1} (hypoxic), and 3 mg L^{-1}. In addition, we calculated the duration of hypoxia for each simulation by counting the number of days when bottom oxygen was less than a threshold value at each grid box. We also calculated the shelf area where hypoxic duration exceeds 50 and 250 d/yr by summing the area of grid cells where hypoxic conditions (DO $<$ 2 mg L^{-1}) last for more than 50 and 250 days in year 2007, respectively. We calculated the value of the maximum Brunt-Vaisala Frequency (N^2) as a measure of the stratification strength [*Pond and Pickard*, 1983] for each grid box. We further calculated averaged stratification (maximum N^2 value) by first spatially averaging the N^2 value over the shelf and then averaging over the entire summer (June–August) and the whole year, respectively. We also quantified the extent of the surface river plume by calculating the daily shelf area with surface water salinity less than 24 and then averaging these values over the entire summer (June–August) and the whole year, respectively, for comparison with other metrics.

3. Results

3.1. Model Validation

Simulated temporal variations and spatial distributions of hypoxia from the different model variants are shown in comparison to the observed hypoxic extent in July in Figures 5 and 6, respectively. Despite their

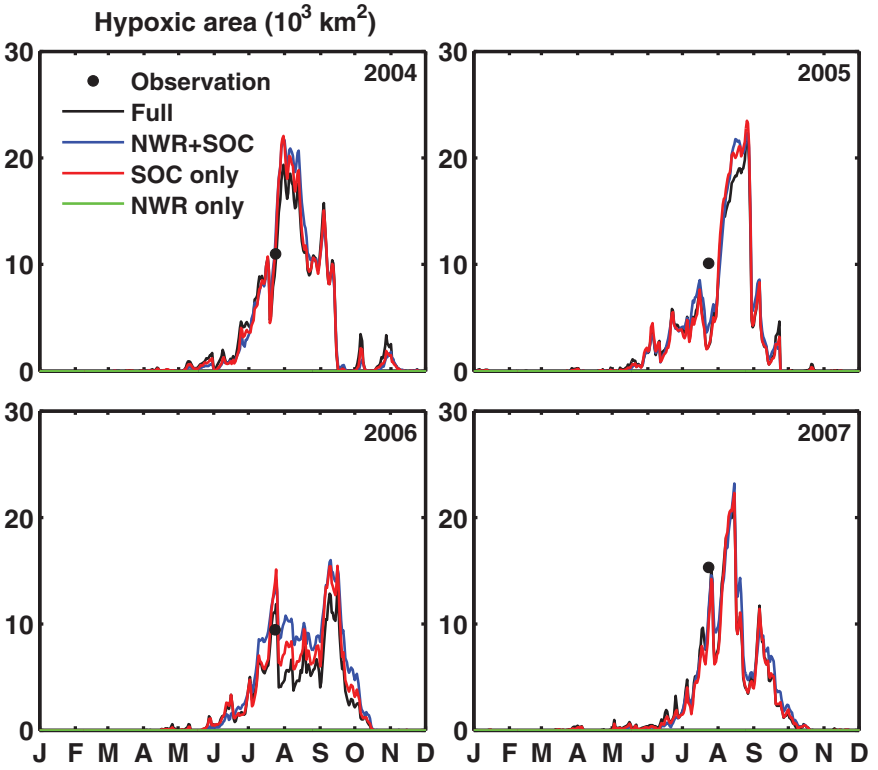

Figure 5. Time series of simulated hypoxic extent (i.e., the area with oxygen concentrations below 62.5 mmol m^{-3} or 2 mg L^{-1})) for the full biogeochemical model (black line), the NWR+SOC model (blue line), the SOC only model (red line), and the NWR only model (green line). Also shown is the observed hypoxic extent in late July (black dots). The observed hypoxic extent was estimated by linearly interpolating the observed oxygen concentrations onto the model grid and then calculating the area with oxygen concentrations below the hypoxic threshold [*Fennel et al.*, 2013].

simplicity, both NWR+SOC and SOC models simulate temporal variations (Figure 5) and spatial distributions of hypoxia (Figure 6) that are very similar to those of the full biogeochemical model, with the two simple oxygen models producing only a slightly larger hypoxic area in summer. Comparison of the NWR+SOC and the SOC models illustrates the effect of turning off the oxygen term in the water column. The difference is small indicating that the net water column respiration rate (NWR) only slightly increases the simulated hypoxic area. The NWR simulation shows that without sediment oxygen consumption the model does not produce any hypoxia at all (Figure 5). Therefore we do not present any further results from the NWR simulation.

Figure 7 shows profiles of bias between simulated and observed oxygen profiles in summer months. Overall, the model-data biases are often within one standard deviation of the observations. The full biogeochemical model generally overestimates the observed oxygen throughout the water column, whereas the two simple oxygen models mostly underestimate the observations in the upper layers but overestimate them in the lower layers (except in the Mississippi Intermediate region in August and Mid-shelf region in June and July). Of the three model simulations, NWR+SOC simulates the lowest oxygen values and agrees best with observed oxygen in bottom layers except in the Atchafalaya plume and Mid-shelf region in June and July. Since we are most interested in the oxygen concentrations in bottom layers where hypoxia develops, we will focus on comparisons between NWR + SOC and the full biogeochemical models for the remainder of the manuscript.

Figure 8 shows a comparison between the simulated and observed oxygen concentrations at station C6. Both the full biogeochemical model and the NWR+SOC model reproduce the observed vertical distribution in oxygen concentrations and seasonal drawdown of oxygen in summer and the subsequent ventilation in the fall. The surface and bottom oxygen concentrations are similar in winter when the water column is well mixed, but they greatly diverge from each other in summer when strong stratification isolates the oxygen-rich surface waters from the oxygen-poor bottom waters (Figure 8, bottom). The simulated oxygen distribution of the NWR+SOC model is almost identical to that of the full model, except that the former produces

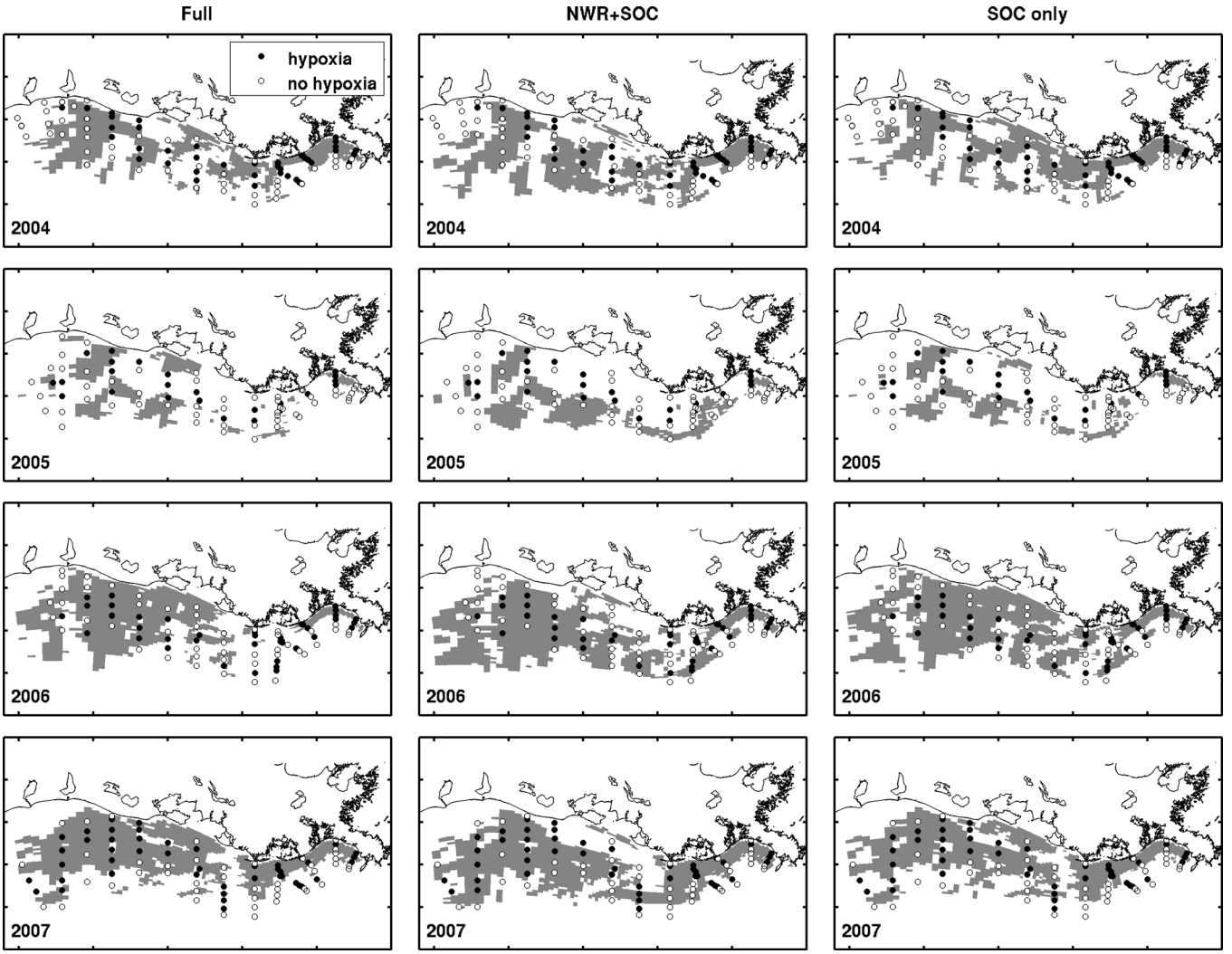

Figure 6. Simulated (gray areas) and observed (dots) hypoxic conditions from the full biogeochemical model (left column), the NWR+SOC model (middle column), and the SOC only model (right column) for the years 2004–2007. The simulated hypoxic area includes all bottom grid boxes where dissolved oxygen < 62.5 mmol m^{-3} during the July monitoring cruise. The stations where hypoxia was observed are shown as filled black dots, while stations without hypoxia are shown as open dots.

slightly lower oxygen concentrations throughout the water column and does not capture the observed supersaturation of surface oxygen during spring and summer. Profiles of bias between simulated and observed oxygen at station C6 (supporting information Figure S1) show that both models underestimate observations in the upper half of the water column and overestimate observations in the lower half of water column; however, compared with the full model, the NWR+SOC model underestimates the observed oxygen more in the upper layers (i.e., surface layer biases are -0.65 and -0.72 mg L^{-1} for the full and the NWR+SOC models, respectively) but overestimates the observed oxygen less in the lower water layers (bottom layer biases are 1.19 and 0.84 mg L^{-1}, respectively).

A comparison between the simulated and observed summer and nonsummer average oxygen concentrations along the C transect is shown in Figure 9. Both the full biogeochemical model and the NWR+SOC model capture the observed vertical differences in average oxygen for all stations along the C transect and cross-shore variations in the oxygen distribution. The models also capture the seasonality of those differences but generally underestimate the observations in the upper water column in nonsummer months (see supporting information Figure S2, biases in the top 5 m range from -1.54 to -0.03 mg L^{-1} and -2.15 to -0.06 mg L^{-1} for the full and NWR+SOC models, respectively) while overestimating observations in the lower water column in summer (biases in the bottom layer range from 0.63 to 3.15 mg L^{-1} and 0.57 to 1.72 mg L^{-1} for the full and NWR+SOC models, respectively). Compared to the full model, the NWR+SOC

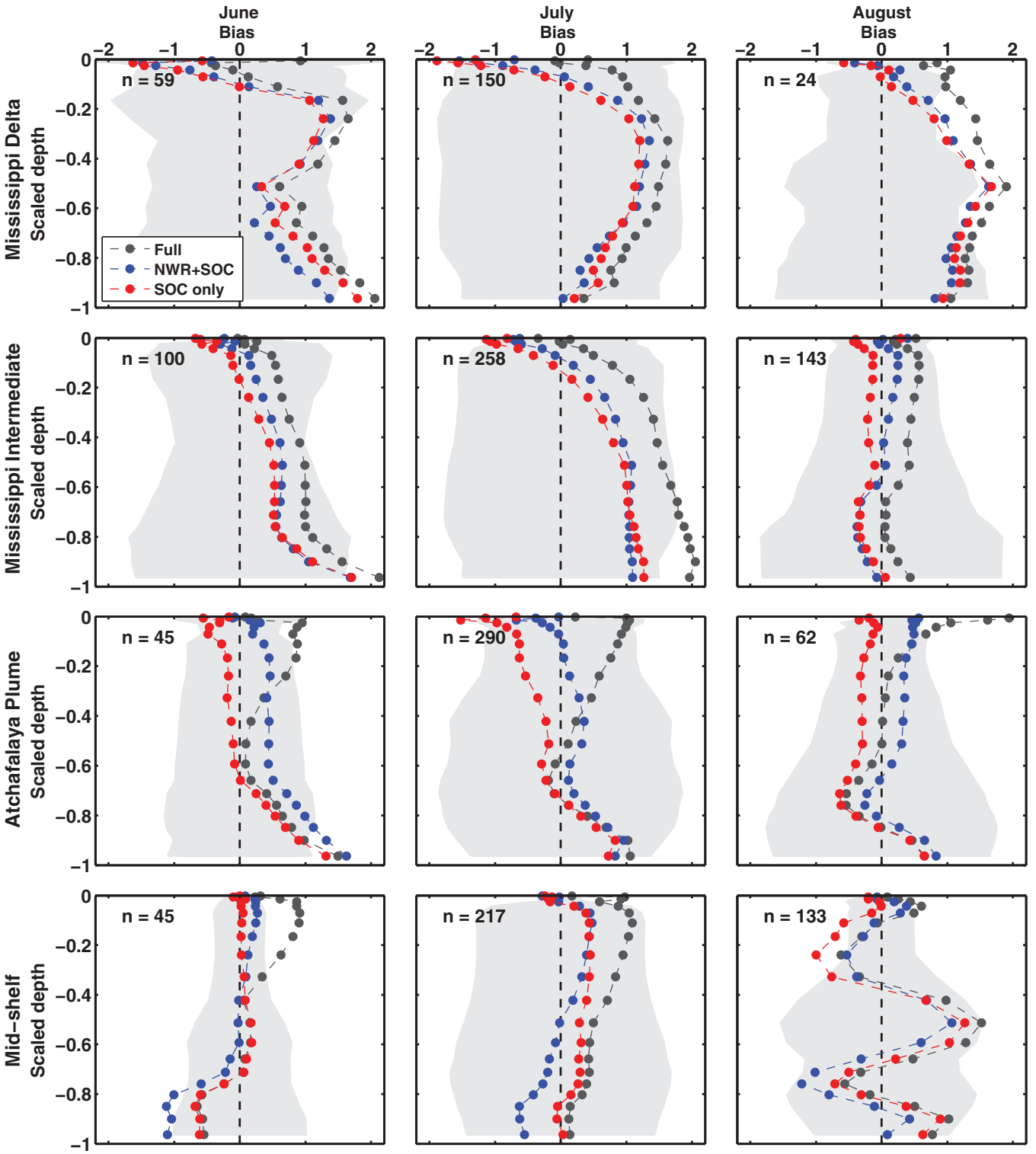

Figure 7. Vertical profiles of model bias (model minus observations, mmol O_2 m^{-3}) in dissolved oxygen (DO) from June to August in 2004–2007 in the four subareas. The vertical axis is the scaled depth, where 0 and −1 represent surface and bottom, respectively. The light shadows represent the one standard deviation in the observations. Observations are from LUMCON [*Rabalais et al.*, 2007], EPA [*Lehrter et al.*, 2009, 2012], *Murrell et al.* [2013a], and MCH.

model simulates slightly lower oxygen concentrations in summer months within the whole water column and hence has relatively larger underestimation of the observed oxygen within the upper 5 m of the water column but smaller overestimation of the observed oxygen in the water column below 5 m.

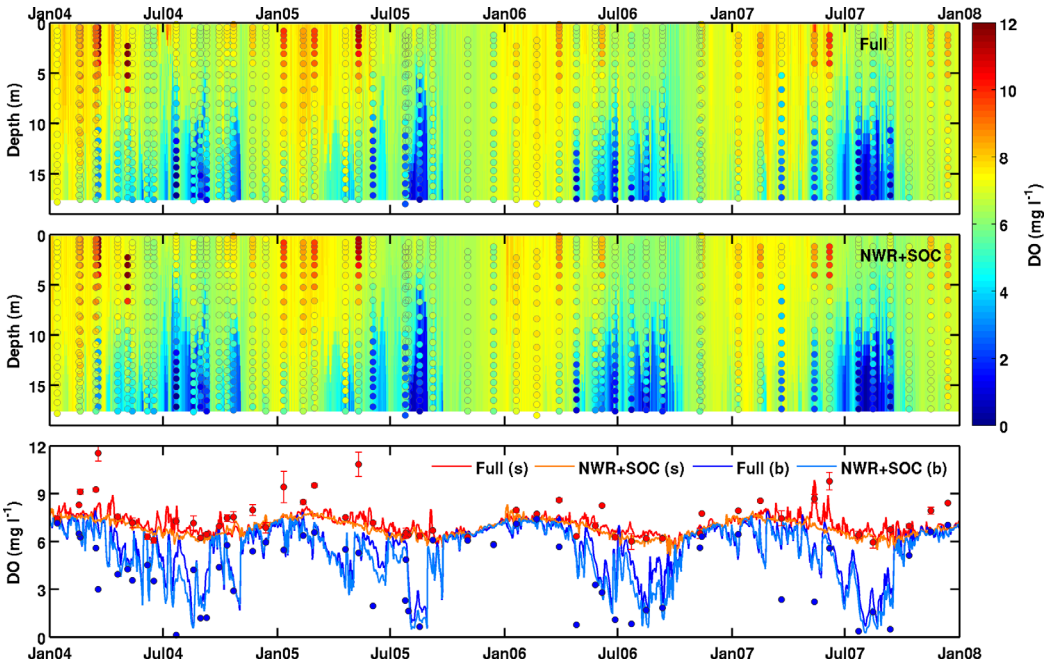

Figure 8. (top) Comparison between the simulated (color map) and observed (colored dots) DO concentrations at station **C6** for full biogeochemical model (top) and the simple NWR+SOC model (middle). (bottom) Comparison between the simulated surface (thick lines) and bottom (thin lines) DO concentrations at station C6 for the full biogeochemical model (black) and the simple NWR+SOC model (gray). Also shown are observations of surface DO averaged over top 5 m layer (red spots with error bars indicating standard deviations) and bottom DO concentrations (blue spots).

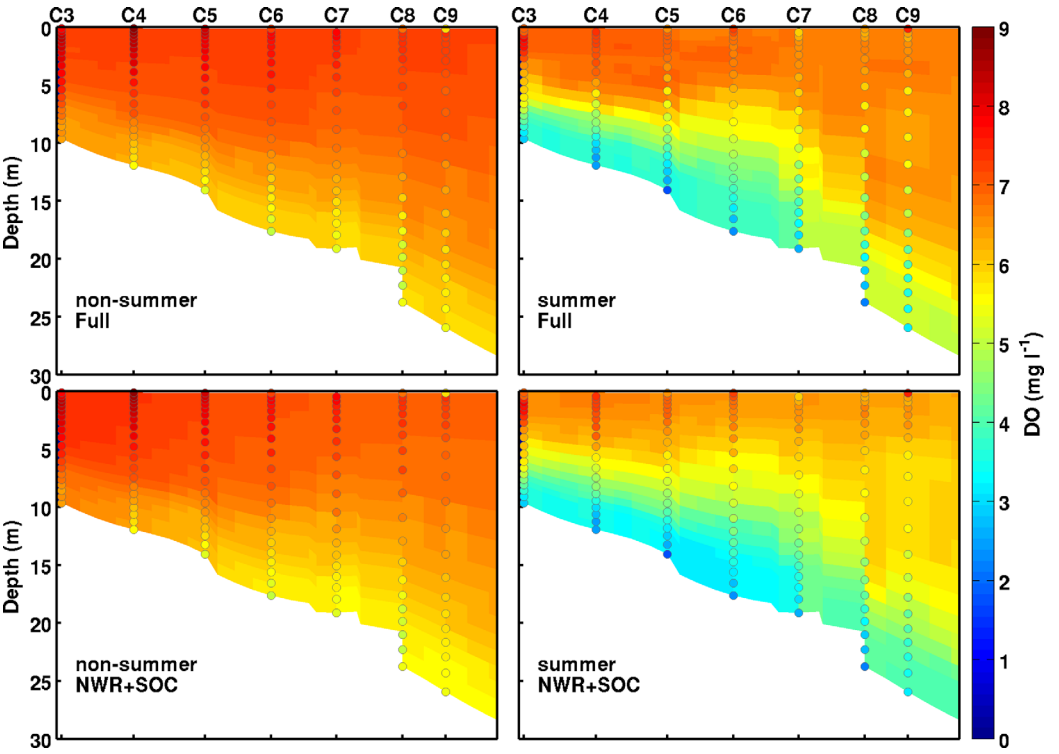

Figure 9. Comparison between the simulated (color map) and observed (dots) seasonal average DO concentrations along the C transect for the full biogeochemical model (top) and simple NWR+SOC model (bottom).

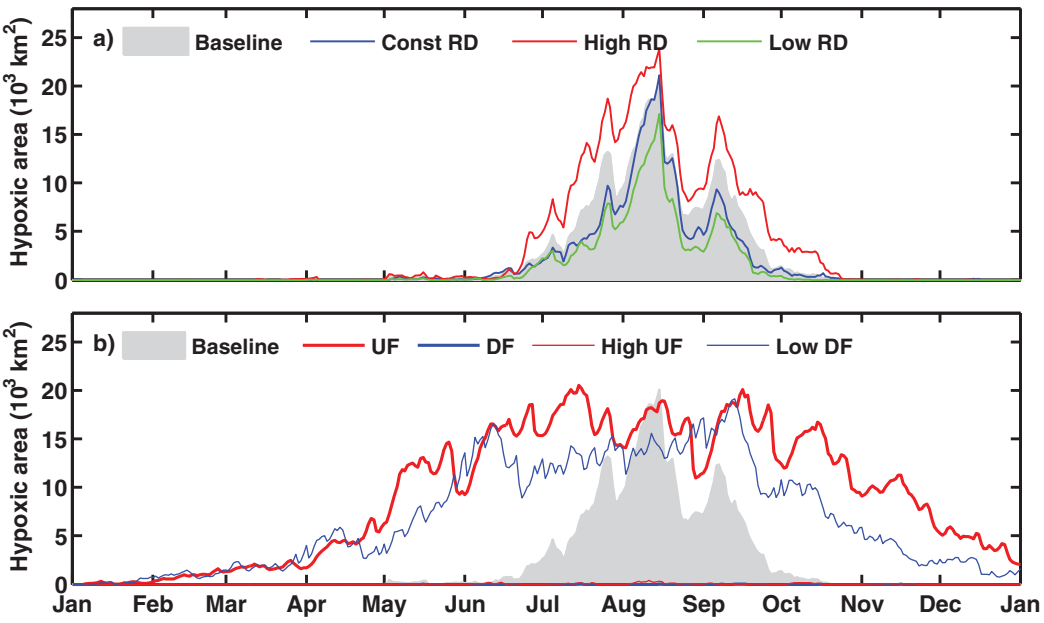

Figure 10. Comparison of the simulated hypoxic area for the baseline run (shaded gray area) with (a) river discharge runs (Const RD: blue line; High RD: red line; Low RD: green line) and (b) wind runs (UF: thick red line; DF: thick blue line; High UF: thin red line; Low DF: thin blue line).

3.2. Response of Hypoxia and Stratification to River Discharge and Wind Forcing

3.2.1. River Discharge

The simulated temporal variations in hypoxic area in the Const RD run are almost identical to those of the baseline run (Figure 10a), with the former simulating lower hypoxic areas (a 15–36% decrease in integrated hypoxic area for different hypoxia thresholds, see Table 3). Doubling the river discharge increases the total integrated hypoxic area by up to 145% for the lowest hypoxia threshold. Halving the river discharge reduces the total integrated hypoxic area by up to 64%. Also noticeable in Table 3 is that the proportional changes of integrated hypoxic area are more pronounced for the more stringent threshold values of hypoxia.

The duration of hypoxia (bottom oxygen < 2 mg L^{-1}) for each simulation is shown in Figure 11. Compared with the baseline run, holding river discharge constant reduces the duration of hypoxia on the western shelf (Figure 11d). Doubling river discharge leads to a westward extension of persistent hypoxia (hypoxia lasting more than 50 days a year) (Figure 11e) and increases the area experiencing persistent hypoxia by 215% above the baseline run, whereas halving river discharge restricts persistent hypoxic condition to the eastern shelf (Figure 11f) and decreases the area experiencing persistent hypoxia by 46% relative to the baseline run (Table 4).

Table 3. Integrated Hypoxic Areas Simulated by Different Model Runs in 2007[a]

	Integrated Hypoxic Area (10^3 km^2 days)			
Model Run	< 0.5 mg L^{-1}	<1 mg L^{-1}	< 2 mg L^{-1}	< 3mg L^{-1}
Baseline	140.1	364.0	820.7	1390.2
Const RD	89.8 (−36%)	261.2 (−28%)	656.1 (−20%)	1181.1 (−15%)
High RD	**343.3 (+145%)**	**666.3 (+83%)**	**1254.5 (+53%)**	**1927.5 (+39%)**
Low RD	50.7 (−64%)	161.6 (−56%)	479.5 (−42%)	955.6 (−31%)
UF	**946.9 (+576%)**	**1861.8 (+411%)**	**3383.4 (+312%)**	**4934.3 (+255%)**
DF	0.0 (−100%)	0.0 (−100%)	0.3 (−100%)	3.1 (−100%)
High UF	0.1 (−100%)	0.8 (−99%)	10.0 (−98%)	51.9 (−96%)
Low DF	**403.5 (+188%)**	**1045.1 (+187%)**	**2517.4 (+207%)**	**4255.9 (+206%)**

[a]For each model run, the total area of water with dissolved oxygen concentration below 0.5 mg L^{-1} (anoxic), 1 mg L^{-1} (strongly hypoxic), 2 mg L^{-1} (hypoxic) and 3 mg L^{-1} was calculated at each day and integrated over all days in 2007. The percentage change relative to the Baseline model run is calculated for each model run ([model-Baseline]/Baseline) and presented in parenthesis. For clarity, increases relative to the Baseline model run are highlighted in bold.

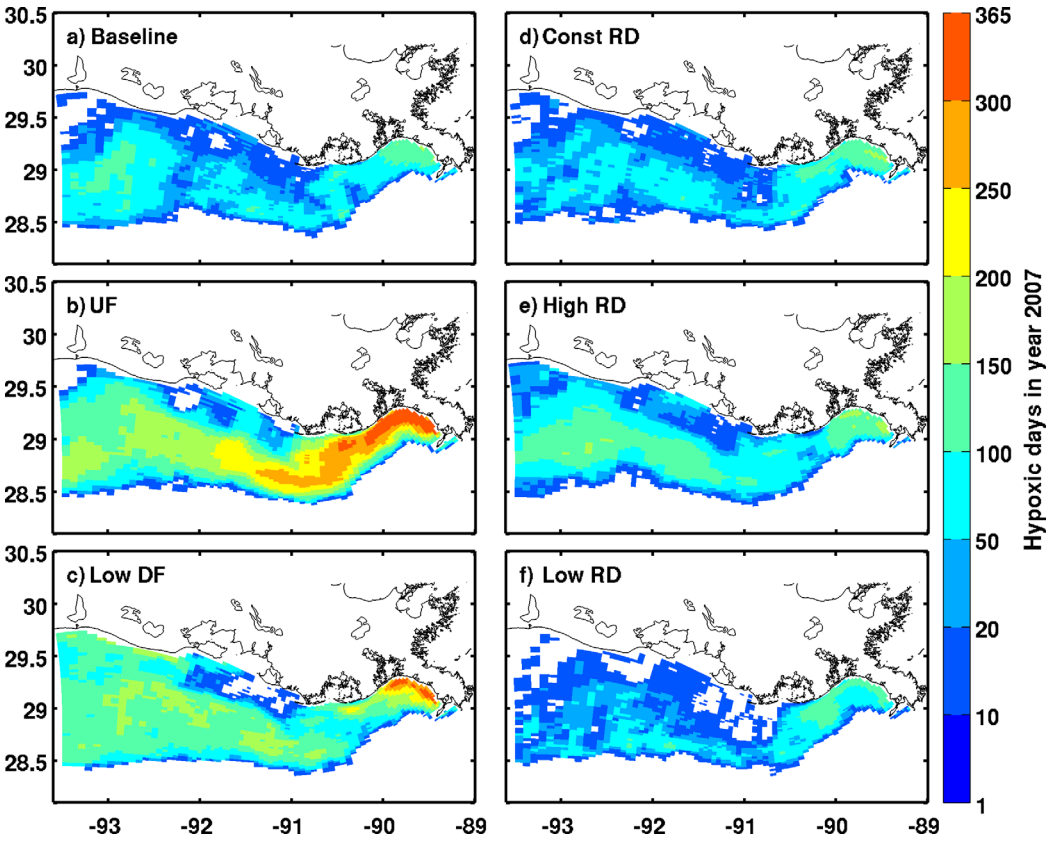

Figure 11. Simulated number of hypoxic days for each model run. The value is calculated at each model grid by counting the number of days when bottom DO < 2 mg L^{-1} (or 62.5 mmol m^{-3}) in year 2007.

The shelf-averaged stratification changes markedly with the changes in river discharge (Figure 12). Doubling or halving the river discharge leads to a significant increase or decrease in the shelf-averaged stratification throughout the year (Figure 12a). The deviation in stratification for the Const RD run relative to the Baseline run (Figure 12d) demonstrates a strong negative correlation ($r=-0.74$) with river discharge (Figure 3) when lagged by 9 days.

Figure 13 further shows that doubling or halving the river discharge, respectively, enhances or reduces stratification over the majority of the shelf in summer months, except in the regions adjacent to the river mouths where stratification goes down with increasing river discharge.

The horizontal and vertical distributions of the river plume under the different river scenarios are shown in Figures 14 and 15, respectively. Increasing the river discharge leads to a large westward and offshore

Table 4. Shelf Area Where Hypoxic Duration Exceeds 50 and 250 d/yr, Average Area of the Surface River Plume (Area of Surface Salinity <=24) and Average Stratification (Maximum N^2) Over Specific Periods for All Model Runs[a]

	Area of DO < 2 mg L^{-1} (10^3 km^2)		Average Area of Surface River Plume (10^6 km^2)		Average N^2 (10^{-3} s^{-2})	
Model Run	Duration>50 d/yr	Duration>250 d/yr	Summer Average	Yearly Average	Summer Average	Yearly Average
Baseline	3.2	0.0	0.9	2.3	15.9	9.2
Const RD	2.0 (−36%)	0.0	0.8 (−13%)	2.2 (−7%)	15.3 (−4%)	9.0 (−2%)
High RD	**10.0 (+215%)**	0.0	**2.1 (+116%)**	**4.8 (+107%)**	**22.0 (+39%)**	**13.3 (+45%)**
Low RD	1.7 (−46%)	0.0	0.4 (−62%)	1.0 (−56%)	9.5 (−40%)	5.4 (−41%)
UF	**23.7 (+647%)**	**1.3**	**1.1 (+11%)**	**4.2 (+78%)**	**18.0 (+13%)**	**17.9 (+95%)**
DF	0.0 (−100%)	0.0	0.3 (−67%)	1.3 (−46%)	4.5 (−72%)	4.4 (−52%)
High UF	0.0 (−100%)	0.0	0.4 (−57%)	1.6 (−31%)	5.3 (−67%)	5.2 (−43%)
Low DF	**24.3 (+667%)**	**0.2**	**1.0 (+4%)**	**3.8 (+64%)**	13.7 (−13%)	**13.0 (+42%)**

[a]The percentage change relative to the Baseline model run ([model-Baseline]/Baseline) is given in parentheses. For clarity, increases relative to the Baseline model run are highlighted in bold.

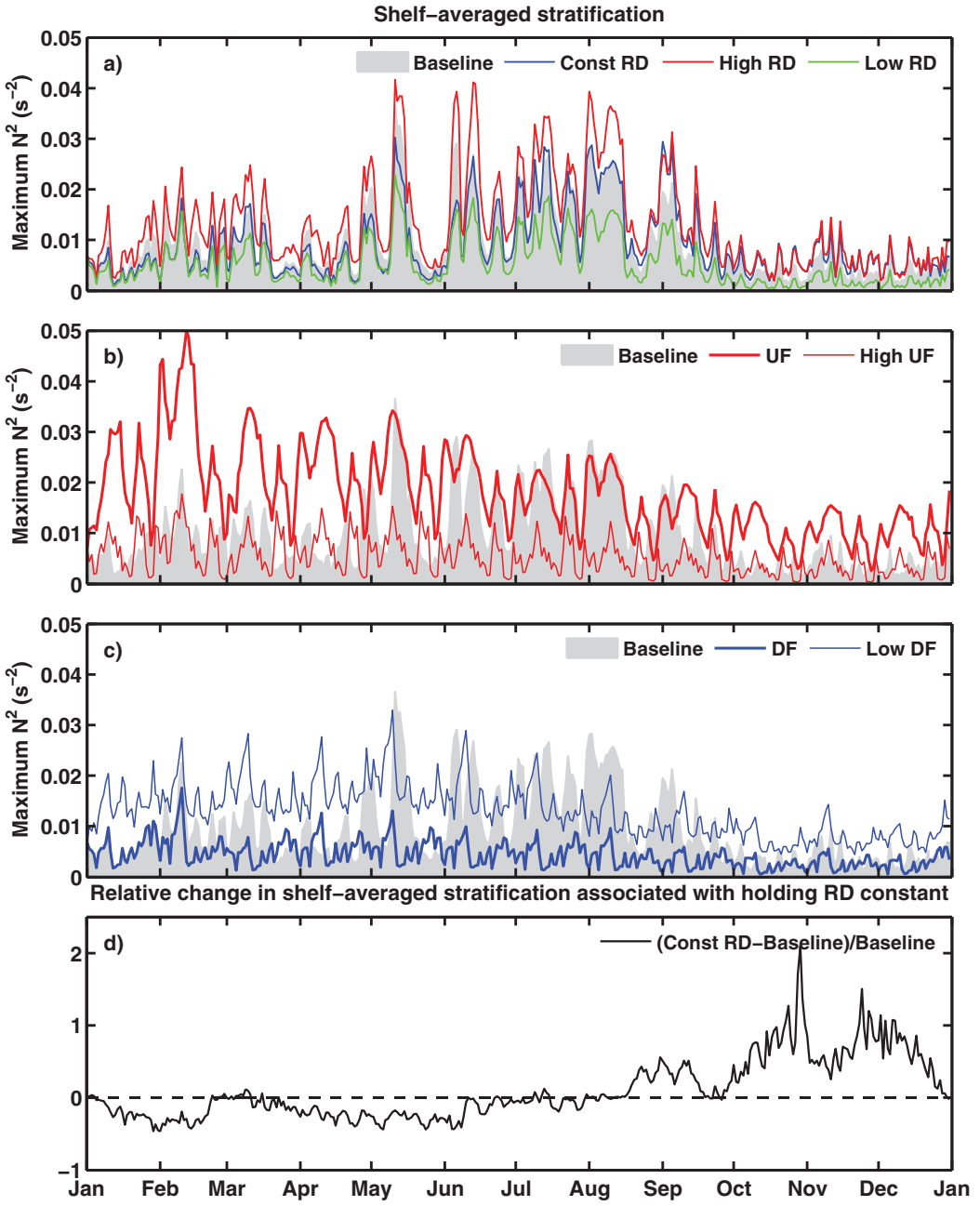

Figure 12. Averaged stratification over the shelf (subregions in Figure 1) for (a) baseline run (gray shadow) and river discharge runs (Const RD: blue line; High RD: red line; Low RD: green line); (b) baseline run (gray shadow) and upwelling-favorable wind runs (UF: thick red line; High UF: thin red line); (c) baseline run (gray shadow) and downwelling-favorable wind runs (DF: thick blue line; Low DF: thin blue line); (d) relative change in shelf-averaged stratification associated with holding river discharge constant ((Const RD-Baseline)/Baseline). Positive values indicate higher stratification for Const RD run than baseline run.

extension of the lighter, fresher plume water, where the isohalines are almost parallel to the coast (Figure 14c) and are significantly tilted offshore (Figure 15c). In contrast, decreasing river discharge confines the plume water to near the river mouths (Figure 14d), which can also be observed in the vertical section where the 24 isohaline is pushed toward the shore and is less tilted than in the baseline run (Figure 15d).

The metrics reported in Table 4 further show that variations in river discharge markedly affect the average area of the surface river plume (salinity < 24), average shelf stratification, hypoxic area (Table 3), and the duration of persistent hypoxia.

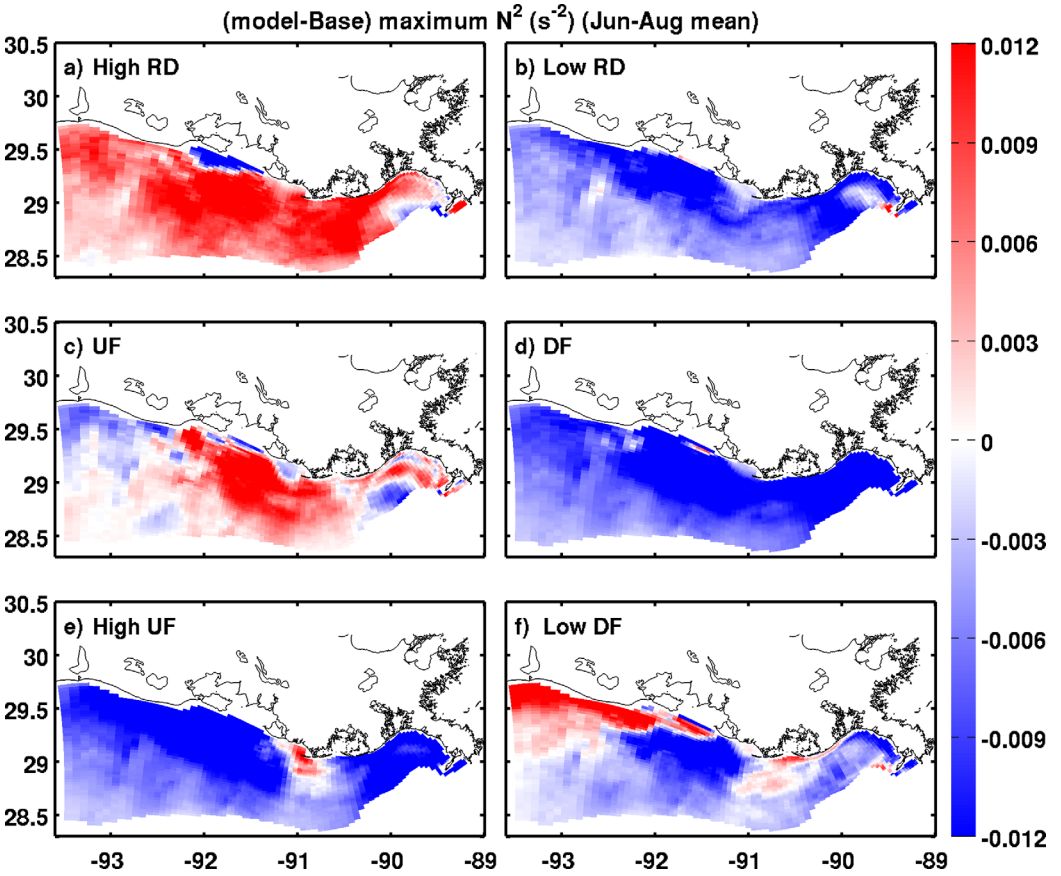

Figure 13. The deviation in summer averaged stratification from the baseline model run (model - Baseline). Stratification is quantified by maximum N^2 value and averaged for the period June–August. Red (positive value) represents higher and blue (negative value) represents lower stratification than the baseline run.

3.2.2. Wind Forcing

Seasonal changes in wind speed and direction strongly influence the seasonal cycle of the simulated hypoxic area (Figure 10b). In the baseline run, hypoxia develops from June to September when wind direction switches to upwelling-favorable and wind speed is relatively low, and it shrinks and disappears for the rest of the year. In the UF wind run where light, upwelling-favorable wind conditions are imposed all year, extensive hypoxic conditions begin in January and persist through the year, and the integrated hypoxic area increases by roughly a factor of 2.6–5.8 compared to the baseline run (Table 3). In contrast, when strong, downwelling-favorable winds are imposed all year in the DF run, essentially no hypoxia is simulated.

Increasing the speed of upwelling-favorable wind in the High UF run essentially eradicates hypoxia, similar to the DF wind case (Figure 10b). Decreasing the speed of downwelling-favorable wind in the Low DF run produces extensive hypoxia throughout the year, similar to the UF wind case; however, the simulated hypoxic area in the Low DF run is smaller than in the UF wind run (Figure 10b).

The geographic distributions of hypoxia are also significantly different between the UF wind run and the Low DF wind run. As shown in Figures 11b and 11c and Table 4, both runs result in an expansion of persistent hypoxic conditions over the shelf, with the area of persistent hypoxia, respectively, increased by 6.5 and 6.7 times than that in the baseline run. In the UF wind case, a large area of extreme hypoxic conditions (>250 days within a year) is simulated along the eastern shelf. In the low DF wind case, extreme hypoxic conditions are simulated closer to shore on the eastern shelf.

The shelf-averaged stratification is high for the whole year in the UF and the Low DF wind cases, but is relatively low throughout the year for the High UF and DF wind cases (Figures 12b and 12c). The deviation in summer stratification from the baseline model run under the different wind forcing is shown in Figure 13

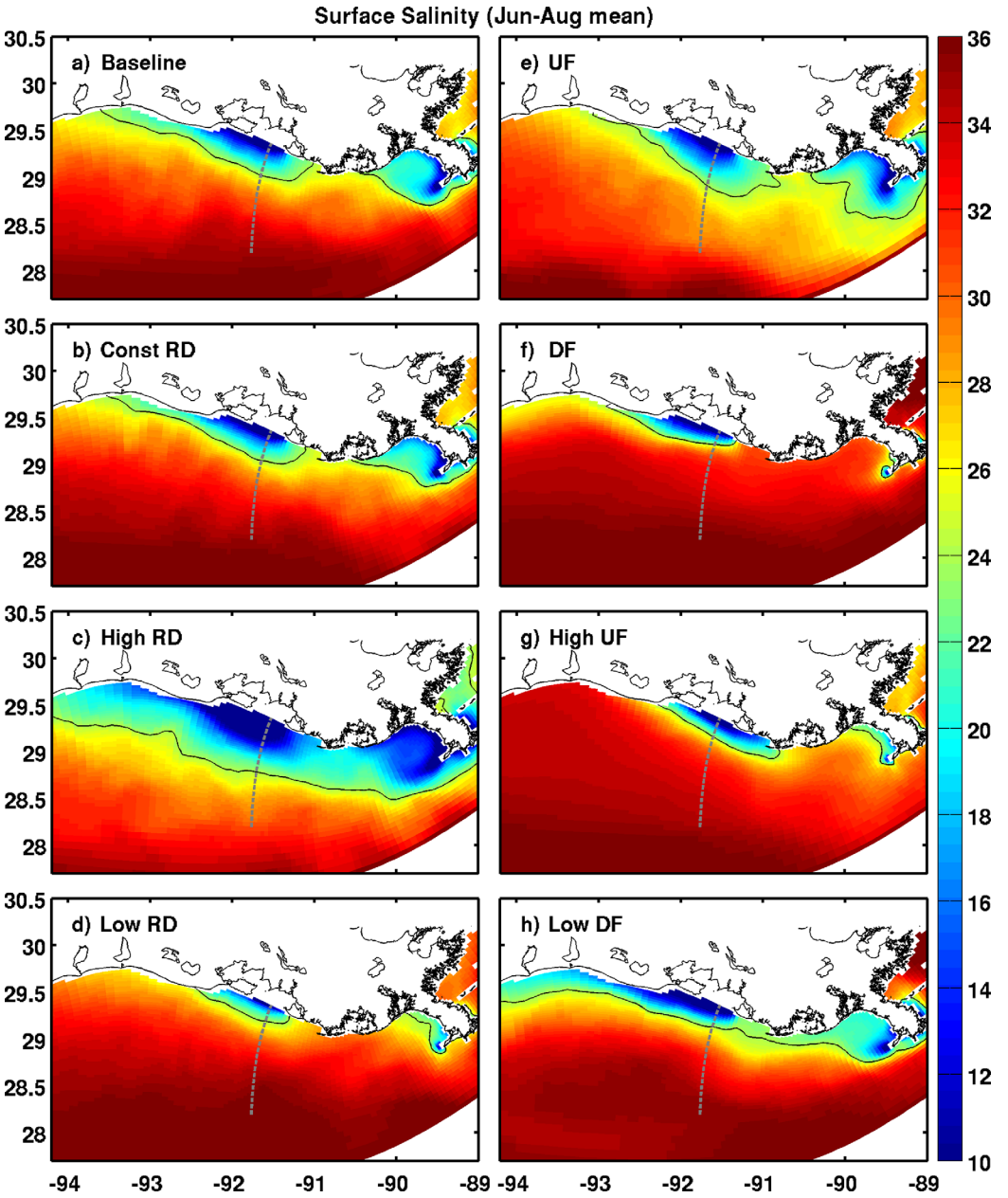

Figure 14. Averaged surface salinity for all model runs. Values are averaged for the period June–August. The black line shows the 24 isohaline. The gray dashed line shows the position of cross-shore transect in Figure 15.

and the shelf-wide average values are summarized in Table 4. The persistent upwelling-favorable wind in UF wind case enhances stratification over the majority of the eastern shelf and in regions offshore, but reduces stratification on the western shelf and in nearshore regions (Figure 14c). The strong downwelling-favorable wind in the DF wind case (Figure 13d) and the increased upwelling-favorable wind in High UF wind case (Figure 13e) both reduce stratification throughout the shelf, except that the latter enhances stratification within a small area near shore around 91°W. Decreasing the downwelling-favorable wind in the Low DF case reduces stratification in river plumes while enhancing stratification on the western shelf and in the portion of the shelf (~91°W) between the Mississippi and Atchafalaya plumes (Figure 13f).

The persistent upwelling-favorable wind in the UF wind case continuously drives freshwater eastward and offshore (Figures 14e and15e). The High UF wind case also drives freshwater eastward and offshore (Figure 14g), but the increased wind speed in this scenario is able to mix the water column more thoroughly (Figure 15g).

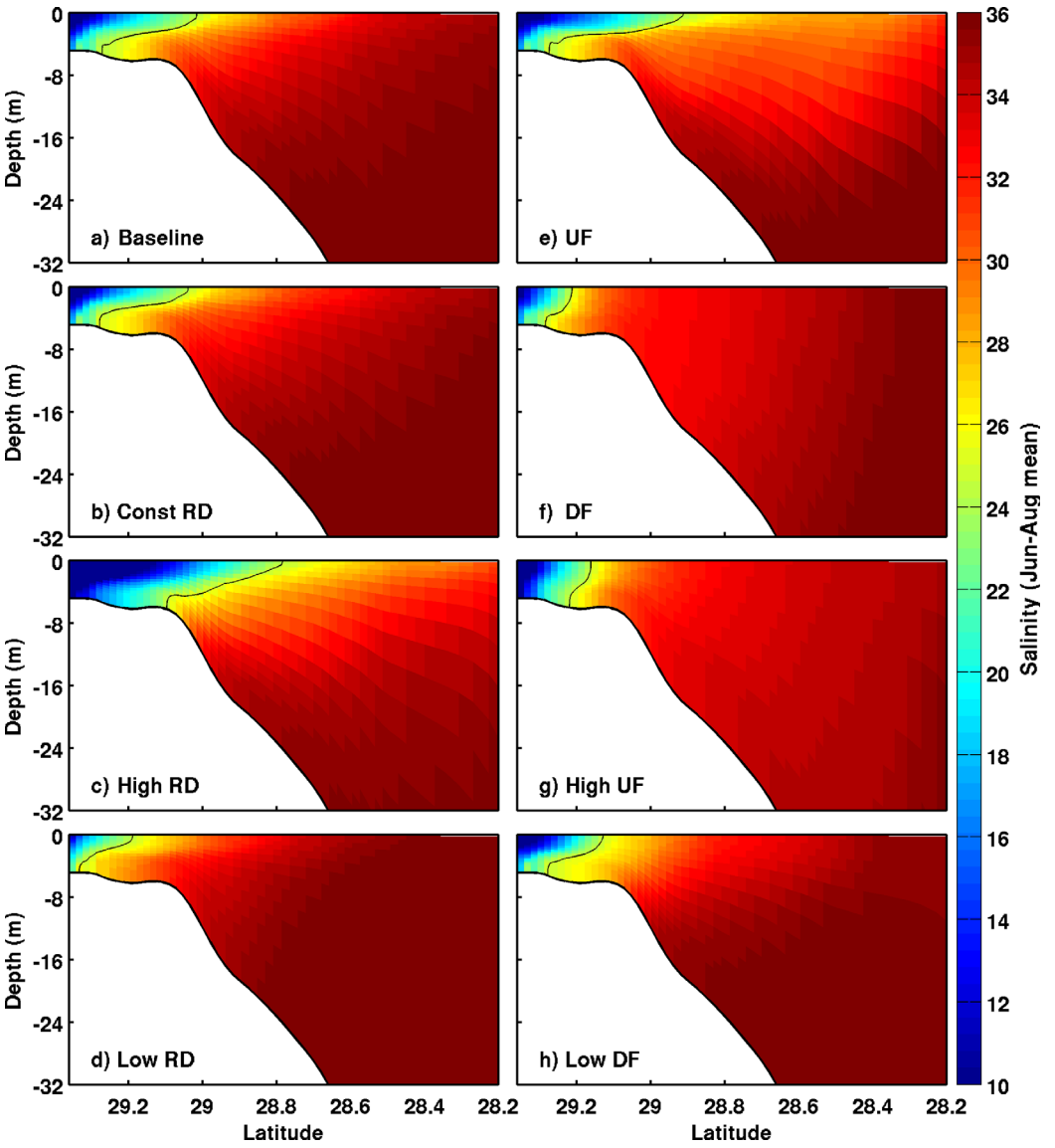

Figure 15. Averaged salinity on a cross-shore transect for all model runs. Values are averaged for the period June–August. The black line shows the 24 isohaline. The position of the transect is shown in Figure 14.

Similarly, the strong downwelling-favorable wind in the DF wind case drives freshwater westward and onshore (Figure 14f), and the wind speed is high enough to mix the water column thoroughly (Figure 15f). Decreasing the downwelling-favorable wind in the Low DF wind case moves light plume water westward and onshore (Figure 14h) but the wind speed is unable to mix the water completely (Figure 15h).

4. Discussion

4.1. Model Validation and Roles of Water Column Versus Sediment Processes

The simple NWR+SOC model closely reproduces the observed temporal variations and spatial distributions of hypoxic extent and oxygen concentrations on the LA shelf when compared to the full biogeochemical model. The NWR+SOC model cannot capture the observed supersaturated oxygen concentrations at the surface due to the lack of biological oxygen production.

Comparison of the NWR+SOC, the SOC, and the NWR simulations illustrates the relative importance of oxygen sinks in water column versus sediment. When turning off the water column oxygen sink, the SOC model simulates an only slightly smaller hypoxic area than the NWR+SOC model does; whereas when

turning off the sediment oxygen consumption, the NWR model does not produce any hypoxia. This confirms that on the LA shelf total oxygen consumption in the bottom layer is more associated with sediment oxygen consumption than water column respiration [*Fennel et al*., 2013], which is in contrast to the situation in Chesapeake Bay [*Li et al*., 2015]. The difference in the dominant type of respiration responsible for producing hypoxia might be due to the differences in geometry and hypoxia structure between the LA shelf and Chesapeake Bay. The LA shelf is largely characterized by a broad and gently-sloping area where hypoxic conditions are restricted to a relatively thin layer above the sediment [*Fennel et al*., 2013]; while the Chesapeake Bay has a relatively deep and narrow central channel isolated by sills and flanked by wide shallow areas, where the dense, low-oxygen waters can accumulate and form a thick hypoxic layer extending tens of meters above the bottom [*Pierson et al*., 2009]. While the importance of local respiration of organic matter to seasonal oxygen decline has been well recognized in other upwelling coastal systems [*Hales et al*., 2006; *Connolly et al*., 2010; *Bianucci et al*., 2011; *Adams et al*., 2013; *Siedlecki et al*., 2014], the relative importance of sediment versus water column respiration to near-bottom hypoxia formation in these systems is still debated. An observational study by *Connolly et al*. [2010] found that biochemical oxygen consumption in the water column and sediments each contribute $\sim$50% to the total oxygen consumption in near-bottom water over the Washington shelf. Using a coupled physical and biogeochemical model, *Bianucci et al*. [2011] demonstrated that remineralization within the sediments, representing $\sim$75% of total oxygen sink, is the dominant process consuming oxygen within the bottom layers on the Vancouver Island shelf. A more recent modeling study by *Siedlecki et al*. [2014] found that sediment oxygen demand is more important in the Washington coast, which has a broad and shallow shelf ($<$ 60 m), whereas water column respiration is more important in recirculation regions such as the Heceta Bank in Oregon coast.

In summary, the fact that the simple oxygen model with a constant oxygen utilization rate in the water column and an oxygen and temperature-dependent sediment oxygen consumption rate can reproduce the observed variability in oxygen concentrations well indicates the important role of physical processes and sediment oxygen sink. The controlling role of sediment oxygen utilization in hypoxia generation on the LA shelf is further demonstrated by the sensitivity experiments disabling oxygen utilization either in the water column or in the sediment. In addition, the ability of the simple oxygen model to closely reproduce the hypoxia evolution of the full biogeochemical model implies that full biogeochemical model may not be necessary for short-term hypoxia forecasting on the LA shelf. However, we would like to note that a full biogeochemical model is necessary to study the effects of varying river nutrient loads on hypoxia and to evaluate the effectiveness of nutrient management strategies [e.g. as in *Laurent and Fennel*, 2014]. Our simple model is appropriate for short-term hypoxia forecasting but not for scenario simulations with varying nutrient loads in this region.

4.2. Model Response to River Discharge and Wind Forcing: From Stratification to Hypoxia

The importance of stratification for the generation of hypoxia has long been discussed [*Wiseman et al*., 1997] and revealed in previous numerical studies [*Hetland and DiMarco*, 2008; *Fennel et al*., 2013]. Using the same circulation model as in this study, *Fennel et al*. [2013] demonstrated that stratification strongly correlates ($r = -0.78$ in year 2007) with the bottom oxygen concentration on the LA shelf. It follows that stratification is an important indicator of oxygen concentration in bottom waters and hence hypoxic conditions. In this section, we discuss how stratification and hypoxia responds to variations in river discharge and wind forcing on the LA shelf.

4.2.1. River Discharge

The simulated seasonal cycle of hypoxia and time-integrated hypoxic area vary significantly with the overall magnitude of river discharge. This can be explained by the significant changes in shelf-averaged stratification associated with the changes in buoyancy inputs. Increasing river discharge leads to an expansion of the lighter, fresher river plume water offshore and westward and an enhancement of shelf-wide stratification, which consequently results in an increase in hypoxic area and the duration of hypoxic conditions over the shelf; whereas decreasing river discharge shrinks the plume, reducing the shelf-wide stratification and thereby significantly decreases the hypoxic area and duration of hypoxia over the shelf. An exception is observed in the regions adjacent to the river mouths where stratification goes down as river discharge increases. We attribute this to the fact that with increased river discharge the freshwater plume is bottom-attached rather then a surface plume and thus less stratified; this is demonstrated in Figure 15c for the High RD run.

The slight difference in simulated seasonal cycle of hypoxic area between the Const RD run and the Baseline run (Figure 10a) suggests that the temporal evolution in river discharge is not an important factor controlling the seasonal cycle of hypoxic area. However, temporal variations in river discharge significantly influence stratification, as suggested by the strong negative correlation between the deviation in stratification for the Const RD run relative to the Baseline run (Figure 12d) and river discharge (Figure 3). A similar result was reported by *Scully* [2013] who used a simple oxygen parameterization with a three-dimensional circulation model in Chesapeake Bay. This is presumably because seasonal bottom oxygen drawdown is the combined result of stratification and oxygen consumption, the latter of which is more associated with the oxygen consumption in sediment than water column on the LA shelf as shown in our model experiments.

Hetland and DiMarco [2008] suggested that stratification sets a physical bound on the region where hypoxia might occur whereas respiratory oxygen consumption associated with organic matter inputs sets the biological bound on the extent and magnitude of hypoxia. In our selected year 2007, the river discharge was mostly above the annual average before June and then decreased to below the annual average for the rest of the year, except for a small rise from mid-July to August (Figure 3). As a result, the most significant deviations in stratification associated with holding river discharge constant occurred in nonsummer months when sediment oxygen consumption was relatively low to form hypoxia (Figure 12d). In other words, while stratification responds quickly to the temporal variability in river discharge, the lack of sufficient oxygen consumption to fuel hypoxia during the same period moderates the impact of temporal variability in river discharge on hypoxia.

4.2.2. Wind Forcing

Using the same realistic biogeochemical model that we used for validation in this study, *Feng et al*. [2013] illustrated how changes in wind associated with changes in the horizontal river plume position affect stratification, primary production, and thereby hypoxia on the shelf. They found that the switch of wind direction to upwelling-favorable directions facilitates hypoxia development, and that the duration of upwelling-favorable wind affects the evolution of hypoxic conditions and the dates when maximum hypoxic extent occurs (e.g., an earlier start of upwelling-favorable wind leads to an earlier maximum extent of the hypoxic area). Our results show that the seasonal changes in wind speed and direction significantly influence the shelf-wide stratification and hence the simulated hypoxia, which are consistent with the mechanism demonstrated by *Feng et al*. [2013], but eliminate the confounding effects of a full biogeochemical model. In our simulations, the persistently weak upwelling-favorable wind continuously expands the lighter and fresher plume water eastward and offshore, which enhances shelf-wide stratification and promotes widespread hypoxia. In contrast, the persistently strong downwelling-favorable wind confines the fresher river plume to the nearshore and the high wind speed homogenizes the water column, reducing stratification and producing essentially no hypoxia throughout the year. Regardless of the wind direction, increasing wind speed destroys the water column stratification and hence decreases hypoxic area, whereas decreasing wind speed enhances water column stratification and hence hypoxic area. This result suggests that changes in wind speed can have a strong impact on stratification and the seasonal cycle of hypoxia.

Despite the similar wind magnitude in the UF wind and low DF wind cases, the stratification in the former is overall stronger than that in the latter case, implying that wind direction can also impact stratification significantly. Moreover, wind direction significantly influences the geographic distribution of the river plume and thereby the geographic distribution of hypoxia. For example, the UF wind case and low DF wind case have similar wind speed, but the UF wind expands the lower-salinity river plume eastward and to the offshore and hence mainly enhances stratification and hypoxic conditions over the eastern shelf and offshore regions; whereas the low DF wind constrains the lower-salinity river plume near the shore and thereby enhances stratification and hypoxia more significantly in near-shore regions.

4.3. Consistency With Observations of Hypoxia

The dominant role of SOC as an oxygen sink in driving hypoxia is consistent with observations by *Quinones-Rivera et al*. [2007], who estimated that SOC accounts for $\sim$73% of the total DO loss within 1 m of the sediments during summer based on δ^{18}O measurements and an isotope fractionation model. Using a different measurement method, *Murrell and Lehrter* [2011] estimated that the benthic respiration only contributes on average 20 $\pm$ 4% of total respiration below the pycnocline. The very large difference in the relative contributions of sediment and water column respiration in these two studies is due to the assumed depth of the bottom layer, as illustrated by *Fennel et al*. [2013] using the same full biogeochemical model as here.

Both *Wiseman et al.* [1997] and *Bianchi et al.* [2010] have demonstrated a strong correlation between the observed mid-summer hypoxic area and the Mississippi River flow. *Bianchi et al.* [2010] further showed that hypoxic area has a similar correlation with either river flow or nutrient loading due to the high correlation between river flow and nutrient loading. Consistent with these studies, our simulations show that the hypoxic area is very sensitive to the magnitude of river discharge. In fact, doubling the river discharge increases the integrated anoxic area (oxygen < 0.5 mg L^{-1}) by 145% while halving the river discharge reduces the integrated anoxic area by 64%. This is also true for the integrated hypoxic area (oxygen < 2 mg L^{-1}) but the changes are smaller. Since our simulation results are based on a model independent of nutrient loading they are not obscured by the effects of nutrient discharge on hypoxic area and isolate the systems response to physical processes.

The impact of wind speed and direction on hypoxia on the LA shelf has already been discussed by *Wiseman et al.* [1997], who found that the low-speed, upwelling-favorable wind during summer drives the river plume eastward and offshore, intensifying stratification and inhibiting the reoxygenation of the near-bottom waters from above. This mechanism described by *Wiseman et al.* [1997] is well reflected by the differences in distribution of the river plume and stratification from our four wind simulations with different wind speeds and directions. Under persistently weak upwelling-favorable wind, the low salinity river plume extends eastward and offshore, enhancing shelf-wide stratification and promoting widespread hypoxia. Under persistently strong downwelling-favorable wind, however, the low salinity river plume is confined to the near-shore and the water column reaches near vertical homogenization, producing essentially no hypoxia. Despite the direction, increasing (decreasing) wind speed weakens (strengthens) water column stratification and hence decreases (increases) hypoxic area on the LA shelf. Wind direction influences the geographic distribution of the river plume and thereby the geographic distribution of hypoxia.

Using a statistical model, *Forrest et al.* [2011] found significant correlation between observed hypoxic area and east-west wind speed. Similarly, *Feng et al.* [2012] showed that the observed hypoxic area significantly correlates with the duration of east-west wind. With a more realistic biogeochemical model as we used for validation in this study, *Feng et al.* [2013] further elucidated the underlying mechanism, namely that wind influenced hypoxia by affecting the vertical and horizontal distribution of low salinity, high chlorophyll plume water on the shelf. Here we took an intermediate approach between the simple statistical model and the more complex biogeochemical model. The coupling of a relatively simple oxygen model to a high-resolution, three-dimensional circulation model in this study allowed us to separate and investigate the effects of wind forcing on the spatial and temporal variability in hypoxia on the LA shelf without the confounding effects of a full biogeochemical model. The model did not capture the observed supersaturated surface oxygen concentrations during spring and summer, which might reduce the vertical oxygen flux through the pycnocline as the oxygen gradient between the upper and lower layers was moderated. But given that we examined the difference between the baseline run and sensitivity runs with different river and wind forcing, our results should not be strongly affected by the slight discrepancy between model and observations.

It is also worth noting that the river discharge and wind forcing ranges used in our model scenarios are not all realistic. The river discharges in the High RD and Low RD runs vary, respectively, around the upper and lower range of the long-term river discharge (1983–2010). The wind scenarios have preserved the event-scale variability but they do not represent realistic seasonal variations in wind forcing over the LA shelf. To assess the impacts of climate change on hypoxia, more realistic model scenarios based on climate projections of river discharge and wind field changes in this region are required.

5. Summary and Conclusions

In this study, we used a three-dimensional circulation model with a relatively simple parameterization of oxygen dynamics to isolate and investigate the effects of physical processes on the development of seasonal hypoxia on the LA shelf. Despite simply assuming a constant biological oxygen utilization rate in the water column and an oxygen and temperature-dependent sediment oxygen consumption rate, the model reasonably reproduces the observed variability of oxygen and the hypoxic area on the LA shelf, highlighting the important role of physical processes. Further, the model sensitivity experiments disabling oxygen

utilization either in water column or in the sediment show that hypoxia generation on the LA shelf is driven by oxygen utilization in the sediment.

Based on the model simulations, the temporal variability in river discharge influences stratification significantly but has less effect on the seasonal evolution of the hypoxic area because oxygen consumption moderates the impact of stratification changes associating with temporal changes in river discharge. The seasonal cycle of hypoxia and integrated hypoxic area are very sensitive to the overall magnitude of river discharge. The increase in total river discharge leads to an offshore and westward expansion of the lighter, fresher river plume and enhances shelf-wide stratification, and thereby greatly increases the hypoxic area over the shelf. In contrast, the decrease in total river discharge shrinks the plume, reducing the shelf-wide stratification and hence significantly decreases the hypoxic area.

Model simulations demonstrate that changes in wind speed have the greatest impact on the seasonal cycle of hypoxia and hypoxic duration. Persistently weak upwelling-favorable winds expand the low-salinity river plume eastward and offshore, enhancing shelf-wide stratification and promoting widespread hypoxia, whereas persistently strong downwelling-favorable winds confine the low-salinity river plume to the nearshore and homogenize the water column, precluding the generation of hypoxia. Regardless of the wind direction, increasing wind speed weakens the water column stratification and hence decreases the hypoxic area, while decreasing wind speed does the opposite. Wind direction significantly influences the geographic distribution of the river plume and thereby the geographic distribution of hypoxia.

The facts that our simple oxygen model essentially reproduces the hypoxia evolution of the full biogeochemical model, and that physical dynamics are key for determining magnitude and distribution of hypoxia has implications for short-term hypoxia forecasting, namely that a full biogeochemical model may not be necessary for this purpose. It follows that prior to using a complex biogeochemical model, one could take an intermediate approach by developing a relatively simple model that parameterizes biological oxygen terms using empirical relationships derived from observations. This is especially the case for regions that have already developed skillful hydrodynamic models.

Acknowledgments
We thank Michael C. Murrell for making the net water column respiration data sets available. We also thank two anonymous reviewers for their constructive comments on this manuscript. This work was supported by NOAA CSCOR grant NA06N0S4780198 and the US IOOS Coastal Ocean Modeling Testbed. NOAA NGOMEX publication 203. Data for this manuscript are available at *Rabalais et al*. [2007], *Murrell et al*. [2013a, 2013b], *Nunnally et al*. [2013], and the Mechanisms Controlling Hypoxia (MCH) program (http://hypoxia.tamu.edu/field-program).

References

Adams, K. A., J. A. Barth, and F. Chan (2013), Temporal variability of near-bottom dissolved oxygen during upwelling off central Oregon, *J. Geophys. Res. Oceans*, *118*, 4839–4854, doi:10.1002/jgrc.20361.

Bianchi, T. S., S. F. DiMarco, J. H. Cowan, R. D. Hetland, P. Chapman, J. W. Day, and M. A. Allison (2010), The science of hypoxia in the Northern Gulf of Mexico: A review, *Sci. Total Environ.*, *408*(7), 1471–1484, doi:10.1016/j.scitotenv.2009.11.047.

Bianucci, L., K. L. Denman, and D. Ianson (2011), Low oxygen and high inorganic carbon on the Vancouver Island Shelf, *J. Geophys. Res.*, *116*, C07011, doi:10.1029/2010JC006720.

Boyer, T. P., J. I. Antonov, H. E. Garcia, D. R. Johnson, R. A. Locarnini, A. V. Mishonov, M. T. Pitcher, O. K. Baranova, and I. V. Smolyar (2006), *World Ocean Database 2005, NOAA Atlas NESDIS 60*, edited by S. Levitus, 190 pp., U.S. Gov. Print. Off., Washington, D. C.

Connolly, T. P., B. M. Hickey, S. L. Geier, and W. P. Cochlan (2010), Processes influencing seasonal hypoxia in the northern California Current System, *J. Geophys. Res.*, *115*, C03021, doi:10.1029/2009JC005283.

da Silva, A. M., C. C. Young-Molling, and S. Levitus (1994a), Anomalies of fluxes of heat and momentum, *Atlas of Surface Marine Data 1994 vol. 3*, NOAA Atlas NESDIS 8, Natl. Oceanic and Atmos. Admin., Silver Spring, Md.

da Silva, A. M., C. C. Young-Molling, and S. Levitus (1994b), Anomalies of fresh water fluxes, *Atlas of Surface Marine Data 1994 vol. 4, NOAA Atlas NESDIS 9*, Natl. Oceanic and Atmos. Admin., Silver Spring, Md.

Feng, Y., S. F. DiMarco, and G. A. Jackson (2012), Relative role of wind forcing and riverine nutrient input on the extent of hypoxia in the northern Gulf of Mexico, *Geophys. Res. Lett.*, *39*, L09601, doi:10.1029/2012GL051192.

Feng, Y., K. Fennel, G. A. Jackson, S. F. DiMarco, and R. D. Hetland (2013), A model study of the response of hypoxia to upwelling-favorable wind on the northern Gulf of Mexico shelf, *J. Mar. Syst.*, *131*, 63–73, doi:10.1016/j.jmarsys.2013.11.009.

Fennel, K., R. Hetland, Y. Feng, and S. DiMarco (2011), A coupled physical-biological model of the Northern Gulf of Mexico shelf: Model description, validation and analysis of phytoplankton variability, *Biogeosciences*, *8*(7), 1881–1899, doi:10.5194/bg-8-1881-2011.

Fennel, K., J. Hu, A. Laurent, M. Marta-Almeida, and R. Hetland (2013), Sensitivity of hypoxia predictions for the northern Gulf of Mexico to sediment oxygen consumption and model nesting, *J. Geophys. Res. Oceans*, *118*, 990–1002, doi:10.1002/jgrc.20077.

Flather, R. A. (1976), A tidal model of the northwest European continental shelf, *Memoires de la Societe Royale de Sciences de Liege*, *10*, 141–164.

Forrest, D. R., R. D. Hetland, and S. F. DiMarco (2011), Multivariable statistical regression models of the areal extent of hypoxia over the Texas-Louisiana continental shelf, *Environ. Res. Lett.*, *6*(4), 045002, doi:10.1088/1748-9326/6/4/045002.

Haidvogel, D. B., et al. (2008), Ocean forecasting in terrain-following coordinates: Formulation and skill assessment of the Regional Ocean Modeling System, *J. Comput. Phys.*, *227*, 3595–3624, doi:10.1016/j.jcp.2007.06.016.

Hales, B., L. Karp-Boss, A. Perlin, and P. Wheeler (2006), Oxygen production and carbon sequestration in an upwelling coastal margin, *Global Biogeochem. Cycles*, *20*, GB3001, doi:10.1029/2005GB002517.

Hetland, R. D., and S. F. DiMarco (2008), How does the character of oxygen demand control the structure of hypoxia on the Texas–Louisiana continental shelf?, *J. Mar. Syst.*, *70*(1-2), 49–62, doi:10.1016/j.jmarsys.2007.03.002.

Hetland, R. D., and S. F. DiMarco (2012), Skill assessment of a hydrodynamic model of circulation over the Texas-Louisiana continental shelf, *Ocean Modell.*, *43–44*, 64–76, doi:10.1016/j.ocemod.2011.11.009.

Justić, D., and L. Wang (2014), Assessing temporal and spatial variability of hypoxia over the inner Louisiana-upper Texas shelf: Application of an unstructured-grid three-dimensional coupled hydrodynamic-water quality model, *Cont. Shelf Res.*, *72*, 163–179.

Laurent, A., and K. Fennel (2014), Simulated reduction of hypoxia in the northern Gulf of Mexico due to phosphorus limitation, *Elem. Sci. Anth.*, *2*(1), 000022, doi:10.12952/journal.elementa.000022.

Laurent, A., K. Fennel, J. Hu, and R. Hetland (2012), Simulating the effects of phosphorus limitation in the Mississippi and Atchafalaya River plumes, *Biogeosciences*, *9*(11), 4707–4723, doi:10.5194/bg-9-4707-2012.

Lehrter, J. C., M. C. Murrell, and J. C. Kurtz (2009), Interactions between Mississippi River inputs, light, and phytoplankton biomass and phytoplankton production on the Louisiana continental shelf, *Cont. Shelf Res.*, *29*, 1861–1872, doi:10.1016/j.csr.2009.07.001.

Lehrter, J. C., D. L. Beddick, R. Devereux, D. F. Yates, and M. C. Murrell (2012), Sediment-water fluxes of dissolved inorganic carbon, O_2, nutrients, and N_2 from the hypoxic region of the Louisiana continental shelf, *Biogeochem.*, *109*, 233–252, doi:10.1007/s10533-011-9623-x.

Li, Y., M. Li, and M. Kemp (2015), A budget analysis of bottom-water dissolved oxygen in Chesapeake Bay, *Estuarine Coasts*, 1–17, doi:10.1007/s12237-014-9928-9.

Murrell, M. C. and J. C. Lehrter (2011), Sediment and lower water column oxygen consumption in the seasonally hypoxic region of the Louisiana continental shelf, *Estuarine Coasts*, *34*, 912–924.

Murrell, M. C., D. L. Beddick, R. Devereux, R. M. Greene, J. D. Hagy, B. M. Jarvis, J. C. Kurtz, J. C. Lehrter, and D. F. Yates (2013a), Gulf of Mexico hypoxia research program data report: 2002–2007, *EPA/600/R-13/257*, 217 pp., U. S. Environ. Protect. Agency, Washington, D. C. [Available at http://tinyurl.com/ko9wj7j.]

Murrell, M. C., R. S. Stanley, J. C. Lehrter, and J. D. Hagy (2013b), Plankton community respiration, net ecosystem metabolism, and oxygen dynamics on the Louisiana continental shelf: Implications for hypoxia, *Cont. Shelf Res.*, *52*, 27–38, doi:10.1016/j.csr.2012.10.010.

Nunnally, C. C., G. T. Rowe, D. C. O. Thornton, and A. Quigg (2013), Sedimentary oxygen consumption and nutrient regeneration in the Northern Gulf of Mexico hypoxic zone, *J. Coast. Res.*, *63*(sp1), 84–96, doi:10.2112/SI63-008.1.

Obenour, D. R., A. M. Michalak, Y. Zhou, and D. Scavia (2012), Quantifying the impacts of stratification and nutrient loading on hypoxia in the northern Gulf of Mexico., *Environ. Sci. Technol.*, *46*(10), 5489–96, doi:10.1021/es204481a.

Obenour, D. R., D. Scavia, N. N. Rabalais, R. E. Turner, and A. M. Michalak (2013), Retrospective Analysis of Midsummer Hypoxic Area and Volume in the Northern Gulf of Mexico, 1985–2011, *Environ. Sci. Technol.*, *47*(17), 9808–9815, doi:10.1021/es400983g.

Obenour, D. R., A. Michalak, and D. Scavia (2015), Assessing biophysical controls on Gulf of Mexico hypoxia through probabilistic modeling, *Ecol. Appl.*, *25*(2), 492–505, doi:10.1890/13-2257.1.

Pierson, J. J., M. R. Roman, D. G. Kimmel, W. C. Boicourt, and X. Zhang (2009), Quantifying changes in the vertical distribution of mesozooplankton in response to hypoxic bottom waters, *J. Exp. Mar. Biol. Ecol.*, *381* S74–S79, doi:10.1016/j.jembe.2009.07.013.

Pond, S., and G. L. Pickard (1983), *Introductory Dynamical Oceanography*, 2nd ed., Pergamon Press, Oxford, U. K.

Quinones-Rivera, Z. J., B. Wissel, D. Justic, and B. Fry (2007), Partitioning oxygen sources and sinks in a stratified, eutrophic coastal ecosystem using stable oxygen isotopes, *Mar. Ecol. Prog. Ser.*, *342*, 69–83.

Rabalais, N. N., R. E. Turner, B. K. Sen Gupta, D. Boesch, P. Chapman, and M. C. Murrell (2007), Hypoxia in the northern Gulf of Mexico: Does the science support the plan to reduce, mitigate, and control hypoxia?, *Estuaries Coasts*, *30*(5), 753–772.

Scully, M. E. (2013), Physical controls on hypoxia in Chesapeake Bay: A numerical modeling study, *J. Geophys. Res. Oceans*, *118*, 1239–1256, doi:10.1002/jgrc.20138.

Siedlecki, S. A., N. S. Banas, K. A. Davis, S. Giddings, B. M. Hickey, P. MacCready, T. Connolly, and S. Geier (2014), Seasonal and interannual oxygen variability on the Washington and Oregon continental shelves, *J. Geophys. Res. Oceans*, *119*, 608–633, doi:10.1002/2014JC010254.

Wanninkhof, R. (1992), Relationship between wind speed and gas exchange over the ocean, *J. Geophys. Res.*, *97*(C5), 7373–7382, doi:10.1029/92JC00188.

Wiseman, W. J., N. N. Rabalais, R. E. Turner, S. P. Dinnel, and A. MacNaughton (1997), Seasonal and interannual variability within the Louisiana coastal current: Stratification and hypoxia, *J. Mar. Syst.*, *12*(1–4), 237–248, doi:10.1016/S0924-7963(96)00100-5.

Yu, L., K. Fennel, A. Laurent, M. C. Murrell, and J. C. Lehrter (2015), Numerical analysis of the primary processes controlling oxygen dynamics on the Louisiana Shelf, *Biogeosciences*, *12*, 1–14, doi:10.5194/bg-12-1-2015.